

# High-Performance 1200-nm InGaAs and 1300-nm InGaAsN Quantum-Well Lasers by Metalorganic Chemical Vapor Deposition

Nelson Tansu, Jeng-Ya Yeh, and Luke J. Mawst, *Senior Member, IEEE*

**Abstract**—In this paper, we present the characteristics of high-performance strain-compensated MOCVD-grown 1200-nm InGaAs and 1300-nm InGaAsN quantum-well (QW) lasers using AsH<sub>3</sub> and U-Dimethylhydrazine as the group V precursors. The design of the InGaAsN QW active region utilizes an In-content of approximately 40%, which requires only approximately 0.5% N-content to realize emission wavelengths up to 1315-nm. Threshold current densities of only 65–90 A/cm<sup>2</sup> were realized for InGaAs QW lasers, with emission wavelength of 1170–1233 nm. Room-temperature threshold and transparency current densities of 210 and 75–80 A/cm<sup>2</sup>, respectively, have been realized for InGaAsN QW lasers with emission wavelength of 1300-nm. Despite the utilization of the highly-strained InGaAsN QW, double-QW lasers have been realized with excellent lasing performance.

**Index Terms**—Diode lasers, InGaAs-GaAs quantum well (QW), InGaAsN-GaAs QW, long-wavelength lasers, QW lasers, strain.

## I. INTRODUCTION

THE DEMAND for higher bandwidth and longer transmission distance has led the pursuit of low cost single-mode 1300–1550-nm transmitter sources. Transmitters based on 1300-nm edge-emitters or vertical-cavity-surface-emitting-lasers (VCSELs) operating at a modulation bandwidth of 10 Gb/s, for the metro application using single mode fiber, allow data transmission up to a distance of 20–30 km [1], [2]. In order to realize low cost (uncooled) 1300–1550-nm-based optical communications systems, high-performance (i.e., temperature insensitive) diode lasers (either in-plane or VCSELs) are needed which operate up to 85 °C. However, conventional InP-based long wavelength diode lasers, at  $\lambda = 1300 - 1550$  nm, are inherently highly temperature sensitive, due to strong Auger recombination, large carrier leakage from the active layer, intervalence band absorption, and a strongly temperature dependent material gain parameter [1], [2].

Another major factor motivating the development of 1.3–1.55- $\mu$ m GaAs-based diode lasers is the ease in forming high quality (Al)GaAs–AlAs distributed Bragg reflectors (DBRs) on GaAs substrates [1], [2]. The ability to fabricate very high quality AlGaAs-based DBRs has allowed the

GaAs-based VCSELs to have performance comparable to GaAs-based in-plane diode lasers.

An attractive approach for achieving long-wavelength laser emission on GaAs substrates is the use of highly-strained InGaAsN [1]–[17] or InGaAs [18]–[24] QWs. The use of a highly-strained InGaAs QW active layer to extend the emission wavelength to 1.20  $\mu$ m was pioneered by Sato, *et al.* [18] and Kondo, *et al.* [20]. The reduction in the bandgap of the InGaAsN materials, pioneered by Kondow *et al.* [1], due to the existence of the N, is also followed by reduction in the compressive strain of the material due to the smaller native lattice constant of the InGaN compound. Since then, many promising results have been demonstrated for 1.3- $\mu$ m InGaAsN-active lasers [1]–[17].

Similar to 1.3- $\mu$ m lasers on InP, recent studies on recombination mechanisms in InGaAsN/GaAs lasers, at 1.3  $\mu$ m, suggest that Auger recombination may also be a dominant recombination processes in this material system [25]. Other studies identify the role of carrier leakage as well as the material gain parameter in the device temperature sensitivity [26]. At present, a detailed understanding of recombination mechanisms, the material gains, and carrier leakage in this material system is still lacking.

The early development of InGaAsN QW lasers employed nearly-lattice-matched low-In content and high N-content InGaAsN QW active regions [1], [2]. Because of the smaller native lattice constant of the InGaN compound, the incorporation of N into the compressively-strained InGaAs material system can result in a nearly lattice-matched InGaAsN QW. Unfortunately, the performance of the early 1200–1300-nm InGaAsN-QW lasers were significantly inferior to the N-free InGaAs-active lasers as well as the conventional 1300-nm InP-based lasers.

Sato *et al.*, of Ricoh Technologies in Japan, proposed the approach of utilizing very high In-content InGaAsN QW active regions [3] grown by metalorganic chemical vapor deposition (MOCVD). The idea proposed was to utilize as high an In-content as possible in the InGaAsN QW, such that only a minimum amount of N is required to push the peak emission wavelength to 1300 nm. By utilizing this approach, Sato *et al.* were able to realize 1300-nm InGaAsN QW lasers with reasonable threshold current density in the order of 0.9–1 kA/cm<sup>2</sup>. Prior to the year of 2001, the best-published 1300-nm InGaAsN QW lasers [4] have been realized with molecular-beam-epitaxy (MBE), resulting in superior lasing performance in comparison to those of MOCVD-grown 1300-nm InGaAsN QW lasers [3], [5]. Only recently, MOCVD-grown 1300-nm InGaAsN QW lasers

Manuscript received February 19, 2003; revised July 28, 2003.

N. Tansu is with the Center for Optical Technologies, Department of Electrical and Computer Engineering, Lehigh University, Sinclair Laboratory, Bethlehem, PA 18015 USA (e-mail: Tansu@lehigh.edu).

J.-Y. Yeh and L. J. Mawst are with the Reed Center for Photonics, Department of Electrical and Computer Engineering, University of Wisconsin-Madison, Madison, WI 53706 USA.

Digital Object Identifier 10.1109/JSTQE.2003.820911

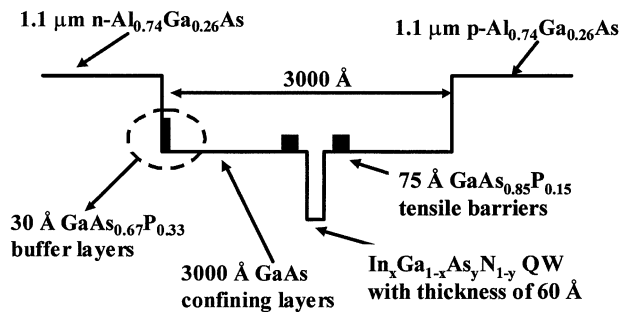


Fig. 1. Cross-sectional schematic conduction band diagram of the  $\text{In}_x\text{Ga}_{1-x}\text{As}_y\text{N}_{1-y}$  QW lasers with tensile-strained  $\text{GaAs}_{0.67}\text{P}_{0.33}$  buffer and  $\text{GaAs}_{0.85}\text{P}_{0.15}$  barrier layers.

[6]–[12] have been realized with performance comparable to the best MBE-grown devices.

This paper deals with various aspects of the lasing characteristics of InGaAs-QW and InGaAsN-QW lasers, grown by low-pressure MOCVD with  $\text{AsH}_3$  as the As-precursor. The InGaAsN QW active structures investigated include both single-QW and double-QW designs with strain compensation from GaAsP tensile-strained barriers. The effect of increased N-content on device performance is also discussed. To clarify the benefits of the InGaAsN QW active region, comparisons with conventional InP-technology is also discussed.

## II. MOCVD-GROWN InGaAs(N) QW

All the lasers structures studied here were grown by low-pressure MOCVD. Trimethylgallium (TMGa), trimethylaluminum (TMAI) and trimethylindium (TMIn) are used as the group III sources and  $\text{AsH}_3$ ,  $\text{PH}_3$ , and U-dimethylhydrazine (U-DMHy) are used as the group V sources. The dopant sources are  $\text{SiH}_4$  and Diethylzinc (DEZn) for the n- and p- dopants, respectively.

A schematic diagram of the laser structure used for both InGaAs and InGaAsN QW active devices is shown in Fig. 1. The growth of the QW, barrier regions, and the optical confinement regions are performed at a temperature of 530 °C. The active regions typically consist of InGaAs and InGaAsN QWs with an In-content of approximately 40% and thickness of 60-Å. The lower- and upper-cladding layers of the lasers consist of  $\text{Al}_{0.74}\text{Ga}_{0.26}\text{As}$  layers with doping levels of  $1 \times 10^{18}\text{cm}^{-3}$  for both the n- and p-cladding layers, respectively. The growth temperatures of the n- and p- $\text{Al}_{0.74}\text{Ga}_{0.26}\text{As}$  are 775 °C and 640 °C, respectively. The annealing of the InGaAsN QW is accomplished during the growth of the top cladding layer at temperature of 640 °C, with duration of approximately 27 min. The InGaAsN QW is surrounded by tensile-strain barriers of  $\text{GaAs}_{0.85}\text{P}_{0.15}$ , which are spaced 100 Å on each side of the QW. The tensile-strained buffer layer consists of a 30-Å  $\text{GaAs}_{0.67}\text{P}_{0.33}$ , which we found to be crucial for the growth of the highly-strained InGaAs(N) QW materials on top of a high Al-content lower cladding layer [6], [7].

One of the challenges in growing InGaAsN QWs with an In-content of 40% by MOCVD is due to the difficulties in incorporating N into the InGaAs QW, while maintaining a high optical quality film. The low purity of the N-precursor used in MOCVD (U-DMHy) is also suspected as a possible

reason for the low optical quality of MOCVD-grown InGaAsN QWs. In order to incorporate sufficient N into the InGaAsN QW, very large  $[\text{DMHy}]/\text{V}$  (as high as 0.961 or high) is required. Due to the high-cost and the low-purity of the DMHy precursor, lowering the  $[\text{AsH}_3]/\text{III}$  to achieve large  $[\text{DMHy}]/\text{V}$  would be the preferable option to increasing the DMHy flow. Large  $[\text{DMHy}]/\text{V}$  ratio requires the  $[\text{AsH}_3]/\text{III}$  ratio to be rather low. Takeuchi *et al.* [15] has demonstrated that the growth of InGaAs QW ( $\lambda = 1200$  nm) with the very low  $[\text{AsH}_3]/\text{III}$  ratio is significantly more challenging compared to the case, in which Tertiary Butyl Arsine (TBA) is utilized as the As-precursor. As the  $[\text{AsH}_3]/\text{III}$  ratio is reduced, the luminescence of the InGaAs QW reduces rapidly for low  $[\text{AsH}_3]/\text{III}$  (below 15–20), which is however required for achieving sufficiently large  $[\text{DMHy}]/\text{V}$ . These challenges have resulted in difficulties in realizing high performance MOCVD-InGaAsN QW lasers with  $\text{AsH}_3$  as the As-precursor until recently [3], [4], [6], [7]. In our approach, the design of the active region is based on strain-compensated InGaAsN QW, with very high In content (In  $\sim 40\%$ ) and minimum N content (N  $\sim 0.5\%$ ), to achieve 1300-nm emission. Minimum N content in the InGaAsN QW allows us to grow the active region with an optimized  $\text{AsH}_3/\text{III}$  ratio. The growth rates for both  $\text{In}_{0.35}\text{Ga}_{0.65}\text{As}_{0.992}\text{N}_{0.008}$  and  $\text{In}_{0.4}\text{Ga}_{0.6}\text{As}_{0.995}\text{N}_{0.005}$  QW active regions are approximately 1.182- $\mu\text{m}/\text{hour}$  and 1.278- $\mu\text{m}/\text{hour}$ , respectively. The  $[\text{AsH}_3]/\text{III}$ ,  $\text{V}/\text{III}$ , and  $[\text{DMHy}]/\text{V}$  ratios for  $\text{In}_{0.4}\text{Ga}_{0.6}\text{As}_{0.995}\text{N}_{0.005}$  QW (and  $\text{In}_{0.35}\text{Ga}_{0.65}\text{As}_{0.992}\text{N}_{0.008}$  QW) active regions are kept at approximately 12 (and 13), 403 (and 437), and 0.969 (and also 0.969), respectively.

All our InGaAs QW [21], [22] and InGaAsN QW [8]–[12] lasers utilize strain-compensation techniques that are based on GaAsP-tensile barrier layers. The utilization of larger bandgap barrier materials will potentially lead to suppression of thermionic carrier leakage, which will in turn lead to a reduction in the temperature sensitivity of the threshold current density of the lasers, in particular at high temperature operation [34].

## III. LASING CHARACTERISTICS OF 1200-nm InGaAs QW

The first step in developing high performance InGaAsN lasers is to establish an optimized growth process for high In-content InGaAs active devices operating near the 1200-nm wavelength region. The addition of small quantities ( $<1\%$ ) of nitrogen can then be used to extend the emission wavelength to 1300-nm.

The  $\text{In}_{0.4}\text{Ga}_{0.6}\text{As}$  QW laser structure studied here uses strain compensation by  $\text{GaAs}_{0.85}\text{P}_{0.15}$  tensile-strained barriers, as shown in Fig. 1. The laser utilizes an active region consisting of a 60-Å  $\text{In}_{0.4}\text{Ga}_{0.6}\text{As}$  QW. From our earlier studies [8], [9], the existence of a slightly tensile-strained buffer layer is found to be essential for the realization of this laser structure. Broad area lasers with a stripe width of 100- $\mu\text{m}$  are fabricated to characterize the device performance under pulsed conditions (pulsewidth of 5  $\mu\text{s}$ , and duty cycle of 1%). The intrinsic physical device parameters can then be extracted from length dependent studies performed on these lasers.

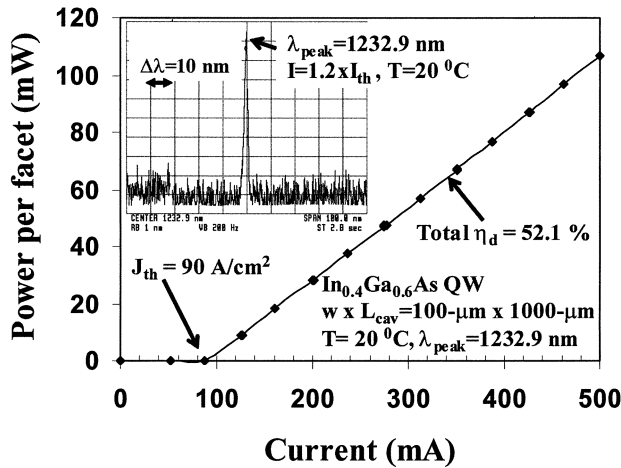


Fig. 2. Relation of output power per facet ( $P$ ) and the total injected current ( $I$ ) for  $\text{In}_{0.4}\text{Ga}_{0.6}\text{As}$  QW lasers with a cavity-length of  $1000\ \mu\text{m}$  at a temperature of  $20\ ^\circ\text{C}$ . The inset shows the lasing spectrum at  $20\ ^\circ\text{C}$ .

The room-temperature ( $T = 20\ ^\circ\text{C}$ ) lasing spectrum for the 60-AA  $\text{In}_{0.4}\text{Ga}_{0.6}\text{As}$  QW devices with cavity length of  $1000\ \mu\text{m}$  is measured to be  $1233\ \text{nm}$ , as shown in Fig. 2. The lasing emission wavelengths range from  $1216$  to  $1233\ \text{nm}$ , with little variation in threshold current densities ( $J_{\text{th}}$ ). As shown in Fig. 2, the threshold current density of these  $\text{In}_{0.4}\text{Ga}_{0.6}\text{As}$  QW lasers are found to be  $90$ – $92\ \text{A}/\text{cm}^2$  for measurements at a heat-sink temperature of  $20\ ^\circ\text{C}$ . The total external differential quantum efficiency ( $\eta_d$ ) of the devices is measured as approximately  $52\%$ .

The temperature characterization of these  $1233\text{-nm}$   $\text{InGaAs}$  QW lasers is conducted from a temperature of  $10\ ^\circ\text{C}$  up to a temperature of  $50\ ^\circ\text{C}$ , with temperature steps of  $5\ ^\circ\text{C}$ . In the temperature range of  $10\ ^\circ\text{C}$ – $50\ ^\circ\text{C}$ , the slope efficiency ( $\eta_d$ ) hardly decreases with temperature, resulting in a  $T_1$  value ( $1/T_1 = (-1/\eta_d) \cdot d\eta_d/dT$ ) of approximately  $1250\ \text{K}$  based on our best fit. It is important to note that  $T_1$  values of  $1250\ \text{K}$  are significantly larger than those of  $1300\text{-nm}$   $\text{InGaAsN}$  QW lasers. For  $1300\text{-nm}$   $\text{InGaAsN}$  QW lasers with the same separate confinement heterostructure as the  $\text{InGaAs}$  active lasers and cavity-length of  $1000\text{-}\mu\text{m}$ , we previously reported  $T_1$  value of  $255\ \text{K}$  for measurements in temperature range of  $20\ ^\circ\text{C}$ – $60\ ^\circ\text{C}$ . The  $T_0$  values ( $1/T_0 = (1/J_{\text{th}}) \cdot dJ_{\text{th}}/dT$ ) are measured as  $140\ \text{K}$ . These reasonably-high  $T_0$  and  $T_1$  values for  $\text{In}_{0.4}\text{Ga}_{0.6}\text{As}$  QW lasers result in very-low threshold-current-densities of only  $160$  and  $190\ \text{A}/\text{cm}^2$  are achieved for devices with cavity-length of  $1000\ \mu\text{m}$  at temperatures of  $85\ ^\circ\text{C}$  and  $100\ ^\circ\text{C}$ , respectively.

Previously, we have reported room-temperature threshold-current-densities of  $65$  and  $100\ \text{A}/\text{cm}^2$  for  $\text{InGaAs}$  QW lasers with emission wavelength of  $1170$  and  $1190\ \text{nm}$ , respectively [21], [22]. The transparency current densities for the  $1170$  and  $1190\text{-nm}$   $\text{InGaAs}$  QW lasers were measured as  $30$  and  $58\ \text{A}/\text{cm}^2$ , respectively, at room temperature [21], [22]. The material gain parameters ( $g_{oJ}$ ) for both the  $1170$ – $1190\text{-nm}$   $\text{InGaAs}$  QW lasers had previously been measured as  $1600$ – $1900\ \text{cm}^{-1}$  [21], [22].

The comparison of the threshold current density ( $J_{\text{th}}$ ) of any QW laser is slightly more challenging, and at times could be deceptive when comparing various laser structures. Threshold current density of a QW laser typically depends on various factors,

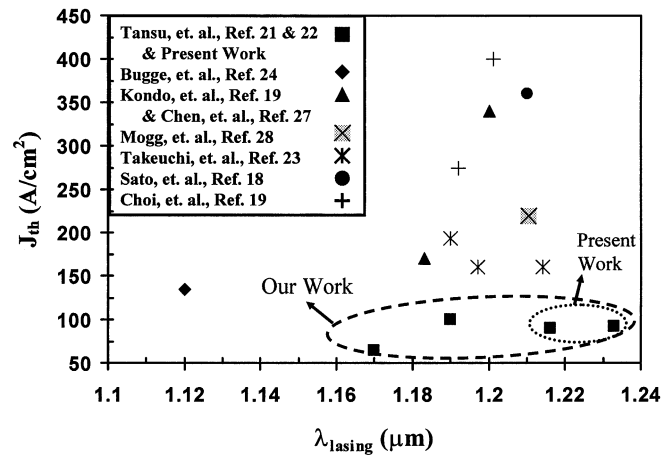


Fig. 3. Comparison of  $J_{\text{th}}$  of  $\text{InGaAs}$  QW lasers in the  $1100$ – $1250\text{-nm}$  wavelength regime.

ranging from the quality of the QW active materials, the gain properties of the QW, the design of the SCH region, the choice of the compositions and doping levels of the cladding layers, and the modal threshold gain. Nevertheless, the comparison of the device performance in term of threshold current density is still of extreme importance, as this is generally the parameter of practical interest for laser diodes.

A comparison of the threshold current density of our  $\text{InGaAs}$  QW lasers with other published results [18]–[24], [27], [28] is shown in Fig. 3. The threshold current densities of the  $1233\text{-nm}$   $\text{In}_{0.4}\text{Ga}_{0.6}\text{As}$  QW ( $L_{\text{cav}} = 1000\text{-}\mu\text{m}$ ) and  $1170\text{-nm}$   $\text{In}_{0.35}\text{Ga}_{0.65}\text{As}$  lasers ( $L_{\text{cav}} = 1500\text{-}\mu\text{m}$ ) are approximately  $90$  and  $65\ \text{A}/\text{cm}^2$ , respectively. To the best of our knowledge, these results represent the lowest reported  $J_{\text{th}}$  values for any QW laser in the wavelength regime of  $1170$ – $1233\ \text{nm}$ . It is also interesting to note that the  $J_{\text{tr}}$  and  $J_{\text{th}}$  of approximately  $30$  and  $65\ \text{A}/\text{cm}^2$  for our  $1170\text{-nm}$   $\text{In}_{0.35}\text{Ga}_{0.65}\text{As}$  QW lasers is comparable with some of the best reported results realized by quantum dot (QD) active lasers in this wavelength regime. The group at the Technical University of Berlin, Berlin, Germany, recently reported QD lasers at an emission wavelength of  $1.15\ \mu\text{m}$  with  $J_{\text{th}}$  and  $J_{\text{tr}}$  of approximately  $100$  and  $20\ \text{A}/\text{cm}^2$ , respectively [29]. The transparency current density in QD lasers is smaller as a result of the smaller active volume of the QDs. Although the  $J_{\text{tr}}$  is smaller, the threshold current density of the QD lasers is not significantly lower than the quantum well (QW) laser, from the fact that the QD active materials have a low material gain parameter. The relatively low  $g_o$  values of QD active material as a result of gain saturation leads to a modal material gain parameter ( $\Gamma_{g_o}$ ) of approximately  $4.5$ – $9\ \text{cm}^{-1}$  per QD stage [30], [31], which is significantly lower than that of the typical  $\Gamma_{g_o}$  for an  $\text{InGaAs}$  QW laser ( $\Gamma_{g_o} = 30$ – $45\ \text{cm}^{-1}$  for an  $\text{InGaAs}$  QW).

#### IV. LASING CHARACTERISTICS OF $\text{InGaAsN}$ QW LASERS

The structure of the  $\text{InGaAsN}$  laser is shown in Fig. 1, which is identical with the structure of  $\text{InGaAs}$  laser except for the active region. The active region utilized here consists of a  $60\text{-}\text{\AA}$   $\text{In}_{0.4}\text{Ga}_{0.6}\text{As}_{0.995}\text{N}_{0.005}$  QW. By utilizing this structure, low-threshold ( $J_{\text{th}}$ ) and transparency- ( $J_{\text{tr}}$ ) current density, strain-

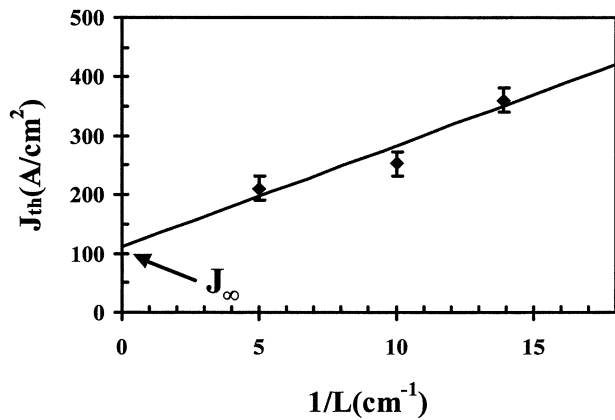


Fig. 4. Room temperature  $J_{th}$  of the  $\text{In}_{0.4}\text{Ga}_{0.6}\text{As}_{0.995}\text{N}_{0.005}$  –  $\text{GaAs}_{0.85}\text{P}_{0.15}$  QW as functions of inverse cavity length ( $1/L$ ).

compensated  $\text{In}_{0.4}\text{Ga}_{0.6}\text{As}_{0.995}\text{N}_{0.005}$  QW lasers with high current injection efficiency ( $\eta_{inj}$ ) were realized.

In characterizing the laser performance of the InGaAsN QW, broad area lasers with stripe widths of  $100\ \mu\text{m}$  are fabricated. The multilength studies of various broad area devices, with cavity lengths ( $L$ ) ranging from  $720$  to  $2000\ \mu\text{m}$ , are utilized to extract the intrinsic device parameters. All the measurements of these broad area devices were performed under pulsed conditions with a pulsewidth of  $6\ \mu\text{s}$ , and 1% duty cycle.

The measured threshold current density, at room temperature ( $20\ ^\circ\text{C}$ ), for the InGaAsN QW lasers, is shown in Fig. 4 for various cavity-length devices. The threshold- and transparency-current density is measured as low as  $211$  and  $79$ – $84\ \text{A}/\text{cm}^2$ , respectively, for devices with cavity length of  $2000\ \mu\text{m}$ , with an emission wavelength of  $1.295\ \mu\text{m}$ . Even for shorter cavity devices of  $500$ ,  $720$ , and  $1000\ \mu\text{m}$ , threshold current densities are measured as low as  $450$ ,  $361$ , and  $253\ \text{A}/\text{cm}^2$ , respectively. To the best of our knowledge, these data represent the lowest threshold- and transparency-current densities reported for InGaAsN QW lasers in the wavelength regime of  $1.28$  to  $1.32\ \mu\text{m}$ .

The external differential quantum efficiency ( $\eta_d$ ) of the InGaAsN QW lasers is as high as 57% for devices with cavity lengths of  $720$ – $\mu\text{m}$ . The lower  $\eta_d$  for the longer cavity devices is attributed to the relatively large internal loss ( $\alpha_i = 10.3\ \text{cm}^{-1}$ ) for these unoptimized structures. The internal loss of the lasers may result from the combination of the narrow SCH region and relatively high doping level ( $1 \times 10^{18}\ \text{cm}^{-3}$ ) of the p-cladding of the laser. By utilizing thin a GaAsP buffer layer in place of InGaP–GaAsP buffer layer [8], improvement in the current injection efficiency ( $\eta_{inj} > 90\%$  –  $95\%$ ) has been achieved as a result of removing the poor-interface between the InGaP-buffer and GaAs-SCH.

The material gain parameter, defined as  $g_{oJ} = g_{th}/\ln(\eta_{inj} \cdot J_{th}/J_{tr})$ , is an important parameter in determining the threshold carrier density ( $n_{th}$ ). Low  $g_{oJ}$  values for a QW laser lead to higher  $n_{th}$ . Higher  $n_{th}$  will result in the possibility of an increase in Auger recombination, due to the  $Cn_{th}^3$  behavior of the Auger recombination rate. Higher  $n_{th}$  will also lead to reduced current injection efficiency, due to a larger recombination in SCH and carrier leakage out of the QW. The material-gain parameter ( $g_{oJ}$ ) [26] and the differential gain ( $dg/dn$ ) [31] of the InGaAsN QW have been shown to

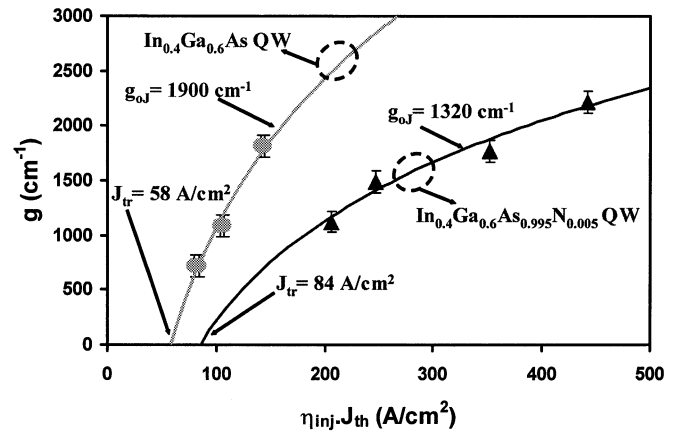


Fig. 5. Gain characteristics of InGaAsN QW and InGaAs QW lasers.

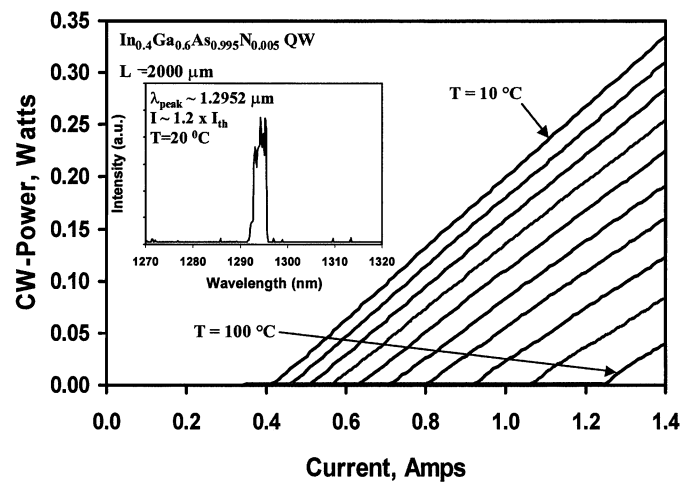


Fig. 6. CW P-I and spectrum of InGaAsN laser with  $L_{cav} = 2000\ \mu\text{m}$ , as a function of temperature.

decrease as nitrogen is introduced into the InGaAs QW. As shown in Fig. 5, the  $g_{oJ}$  of the InGaAsN QW laser is measured as approximately  $1200$ – $1300\ \text{cm}^{-1}$ , which is significantly lower than that ( $g_{oJ} = 1600$  –  $1900\ \text{cm}^{-1}$ ) of similar InGaAs QW lasers [22], [26] at  $\lambda = 1170$  –  $1190\ \text{nm}$ . The InGaAsN active devices, with emission wavelengths of  $1.29$ – $1.295\ \mu\text{m}$ , exhibit relatively low temperature sensitivity with  $T_0$  values of  $82$ – $90\ \text{K}$  for devices with cavity lengths of  $720$ – $2000\ \mu\text{m}$ . The  $T_1$  values are measured to be in the range from  $200$  to  $360\ \text{K}$ , for devices with  $L$  of  $720$ – $2000\ \mu\text{m}$ .

The continuous-wave (CW) operation characteristics of the InGaAsN QW lasers were measured from laser devices with facet coatings of high-reflective (HR) and antireflective (AR) layers. The HR layers consist of three pairs of  $\text{Al}_2\text{O}_3/\text{Si}$  with reflectivity in excess of 95%, and the AR layer was formed by a single layer of  $\text{Al}_2\text{O}_3$  with reflectivity estimated to be in the range 7%–10%. The devices were mounted junction down on copper heatsinks, and they were measured under CW operation for cavity-lengths of  $1000$ – $2000\ \mu\text{m}$  at temperatures in the range of  $10\ ^\circ\text{C}$ – $100\ ^\circ\text{C}$ .

The measured CW output-power ( $P_{out}$ ) characteristics, as a function of the injected-current ( $I$ ) and the heat-sink temperature ( $T$ ), are shown in Fig. 6 The CW measurements of the InGaAsN-QW lasers are measured up to a temperature of  $100\ ^\circ\text{C}$ ,

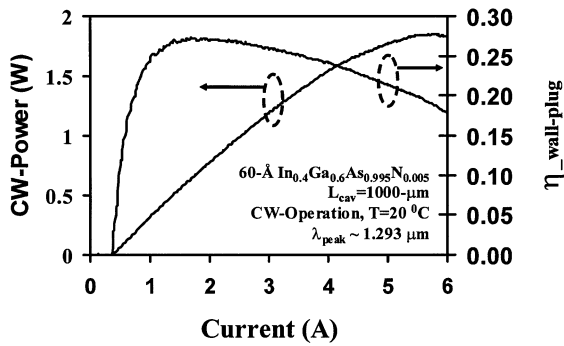


Fig. 7. CW output power characteristics for InGaAsN laser.

limited by our equipment. The near-threshold ( $I \sim 1.2 I_{th}$ ) emission wavelengths of the InGaAsN QW lasers with cavity-length of 2000  $\mu\text{m}$  are measured as approximately 1295.2 and 1331 nm, at a temperature of 20  $^{\circ}\text{C}$  and 100  $^{\circ}\text{C}$ , respectively.

The measured threshold current density of the HR/AR-coated InGaAsN-QW laser devices under CW-operation is very comparable with that of the as-cleaved InGaAsN QW laser devices with cavity length of 2000  $\mu\text{m}$ . Despite the large internal loss of our lasers ( $\alpha_i$  is approximately  $13 \text{ cm}^{-1}$ ), the threshold-current-density of the lasers with cavity-length of 2000  $\mu\text{m}$  is measured as 210–220  $\text{A}/\text{cm}^2$ , at a temperature of 20  $^{\circ}\text{C}$  under CW operation. At elevated temperatures of 80  $^{\circ}\text{C}$  and 100  $^{\circ}\text{C}$ , the threshold current densities of the HR/AR-coated ( $L_{cav} = 2000 - \mu\text{m}$ ) lasers are measured as only 455 and 615  $\text{A}/\text{cm}^2$ , respectively, under CW operation.

The maximum CW output powers achievable from the 1300-nm InGaAsN-QW lasers are approximately 1.8 W for cavity-lengths of both 1000 and 2000  $\mu\text{m}$ , at heat-sink temperatures of 20  $^{\circ}\text{C}$ . Fig. 7 shows the measured output power characteristics for devices with  $L_{cav} = 1000 - \mu\text{m}$ . This result represents the highest CW-output power reported for 1300-nm InGaAsN QW lasers grown by MOCVD at heat-sink temperatures of 20  $^{\circ}\text{C}$ . The maximum wall-plug efficiency for the cavity-length of 1000  $\mu\text{m}$  is approximately 28%, limited by the large internal loss ( $\alpha_i = 13 \text{ cm}^{-1}$ ). Further improvements in the external differential quantum efficiency of InGaAsN QW lasers can be achieved by utilizing a broad waveguide structure to minimize the internal loss.

To compare the lasing performance of the 1300-nm InGaAsN QW lasers with those of the conventional InP-technology, we list the published results that represent among the best-performance 1300-nm diode lasers based on conventional InP technology (InGaAsP-QW [32] and InGaAlAs-QW [33]), as shown in Fig. 8. Due to the low material gain parameter, carrier leakage, and Auger recombination, typically 1300-nm InGaAsP-InP QW lasers require multiple QWs, ranging from 9 to 14 QWs [32]. The 1300-nm InGaAlAs QW requires approximately 4 to 6 QWs for optimized structures [33].

For optimized 1300-nm InGaAsP-QW structures, the threshold current densities of approximately 1650–1700  $\text{A}/\text{cm}^2$  were achieved for devices with cavity-length of 500  $\mu\text{m}$  at operation temperature of 80  $^{\circ}\text{C}$ , as reported by Belenky, *et al.* [32]. The threshold current density of the 1300-nm diode lasers based on the InGaAlAs QW on InP, with cavity-length of 1000  $\mu\text{m}$ , has been reported as approximately 1350  $\text{A}/\text{cm}^2$  at

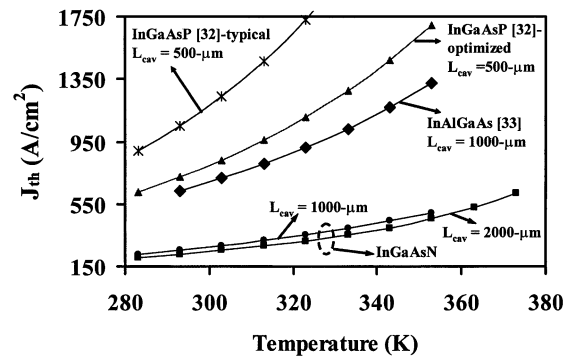


Fig. 8. Comparison of  $J_{th}$  for InGaAsN, AlGaInAs, and InGaAsP active lasers as a function of temperature.

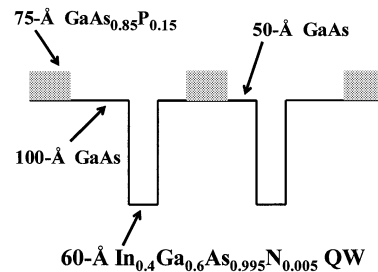


Fig. 9. Schematic energy diagram of the active region for the InGaAsN double-QWs structures.

temperature of 80  $^{\circ}\text{C}$  [33]. The InGaAsN QW lasers require only a single QW active region for high temperature operation, owing to the larger material gain parameter and better electron confinement in the QW. Our 1300-nm InGaAsN single-QW as-cleaved diode lasers, with cavity-length of 500 and 1000  $\mu\text{m}$ , have threshold current densities of only 940 and 490  $\text{A}/\text{cm}^2$ , respectively, at *heat-sink temperature of 80  $^{\circ}\text{C}$* .

## V. 1300-nm InGaAsN DOUBLE-QW LASERS

Typically a single QW is sufficient for application in a conventional edge emitting diode laser. There are other types of devices which require a multiple QW structure as the active region for realizing higher threshold gains and improving the carrier injection efficiency. VCSELs are excellent examples of such devices that require higher gain active regions, due to the significantly higher mirror loss in VCSEL. A concern related to the high In content InGaAs(N) QW is related to the feasibility of implementing several quantum well (MQW) layers without material degradation due to the high strain.

The 1300-nm InGaAsN multiple-QW structure is shown schematically in Fig. 9. The laser structure studied here consists of a 60-A InGaAsN double-QW (DQW) active region, with strain compensation from  $\text{GaAs}_{0.85}\text{P}_{0.15}$  tensile-strained barriers. The optical confinement and the cladding layers of this laser are kept identical to that of the SQW structure shown in Fig. 1. Similar that of the single-QW structure, thermal annealing of the InGaAsN double-QW structure is conducted at 640  $^{\circ}\text{C}$  for a duration of 27 min.

The room temperature lasing spectrum of the InGaAsN-DQW devices with a cavity-length of 1500  $\mu\text{m}$ , was measured at 1315 nm with a  $J_{th}$  of approximately 410  $\text{A}/\text{cm}^2$ . The

slightly longer emission wavelength of the DQW lasers, in comparison to that of the single-QW lasers, can be attributed to smaller quasi-Fermi level separation at threshold. The  $J_{tr}$  and the  $g_oJ$  values for the InGaAsN double-QW lasers are measured as approximately 200 A/cm<sup>2</sup> and 2520 cm<sup>-1</sup>, respectively, as shown in Fig. 12. The scaling of the  $J_{tr}$  and  $g_oJ$  values with number of QWs is in excellent agreement with theory, a good indication of the feasibility to implement highly-strained InGaAsN DQWs for VCSELs structures.

## VI. 1300-nm InGaAsN SINGLE-QW LASERS WITH HIGHER N-CONTENT

The lasing characteristics of 1300-nm InGaAsN QW lasers with higher N-content are fabricated and analyzed for comparison purposes. Higher N-content (0.8%) InGaAsN QW lasers are fabricated using lower In-content (35%) to keep the emission wavelength fixed at 1300-nm. The thickness of the In<sub>0.35</sub>Ga<sub>0.65</sub>As<sub>0.992</sub>N<sub>0.008</sub> single-QW structure is adjusted to approximately 80-Å. The In- and N-compositions are calibrated with SIMS and XRD measurements. In our experiment here, only the active region of the structure, as shown in Fig. 1, is replaced with the 80-Å In<sub>0.35</sub>Ga<sub>0.65</sub>As<sub>0.992</sub>N<sub>0.008</sub> single-QW. The utilization of lower In-content InGaAsN QW active region allows us to increase the thickness of the QW to 80 Å, which would lead to reduction of quantum size effect. Reduced quantum size effect in lower In-content InGaAsN QW will also minimize its N-content requirement to achieve 1300-nm emission wavelength.

The room temperature lasing spectrum of the In<sub>0.35</sub>Ga<sub>0.65</sub>As<sub>0.992</sub>N<sub>0.008</sub> single-QW devices with a cavity-length of 1500 μm, was measured at 1305 nm with a  $J_{th}$  of approximately 417 A/cm<sup>2</sup>. The transparency current density of the 1300-nm In<sub>0.35</sub>Ga<sub>0.65</sub>As<sub>0.992</sub>N<sub>0.008</sub> is estimated as approximately 144 A/cm<sup>2</sup>, which is almost a factor of two higher in comparison to that of the 1300-nm In<sub>0.4</sub>Ga<sub>0.6</sub>As<sub>0.995</sub>N<sub>0.005</sub> single-QW. Approximately 25% of the increase in its  $J_{tr}$  value, in comparison to that of 60-Å In<sub>0.4</sub>Ga<sub>0.6</sub>As<sub>0.995</sub>N<sub>0.005</sub> QW, can be attributed to the 25% thicker dimension of the 80-Å In<sub>0.35</sub>Ga<sub>0.65</sub>As<sub>0.992</sub>N<sub>0.008</sub> QW. The remaining 70%–75% increase in the  $J_{tr}$  value of In<sub>0.35</sub>Ga<sub>0.65</sub>As<sub>0.992</sub>N<sub>0.008</sub> QW lasers, in comparison to that of In<sub>0.4</sub>Ga<sub>0.6</sub>As<sub>0.995</sub>N<sub>0.005</sub> QW, can be attributed to several other factors including increase in monomolecular recombination processes, carrier leakage, or other processes. The material gain parameter ( $g_oJ$ ) of the In<sub>0.35</sub>Ga<sub>0.65</sub>As<sub>0.992</sub>N<sub>0.008</sub> QW is measured as 1265 cm<sup>-1</sup>.

The  $T_0$  and  $T_1$  values of the In<sub>0.35</sub>Ga<sub>0.65</sub>As<sub>0.992</sub>N<sub>0.008</sub> QW lasers are found to be significantly lower in comparison to those of the In<sub>0.4</sub>Ga<sub>0.6</sub>As<sub>0.995</sub>N<sub>0.005</sub> QW lasers, as shown in Figs. 10 and 11, respectively.  $T_0$  and  $T_1$  values of only 75–80 and 100–150 K, respectively, are measured for In<sub>0.35</sub>Ga<sub>0.65</sub>As<sub>0.992</sub>N<sub>0.008</sub> QW lasers with cavity-lengths from 750 to 1500-μm. Careful studies are still required to clarify the mechanisms that lead to the lower  $T_0$  values in these higher N-content InGaAsN QW lasers, in spite of their higher  $J_{th}$ . Possible mechanisms of the lower  $T_0$  and  $T_1$  values include the increase in carrier leakage from a reduction in the

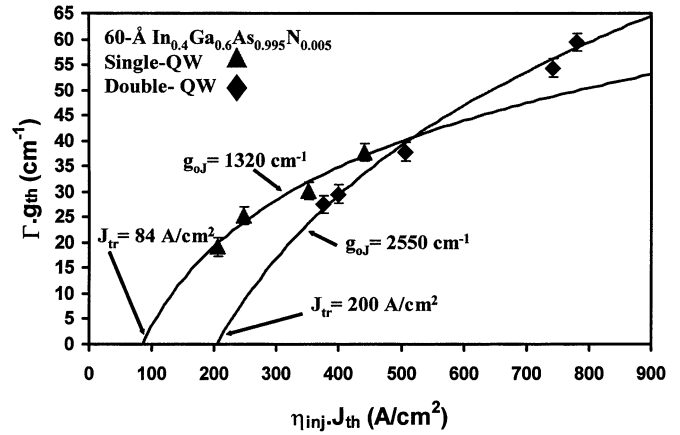


Fig. 10. Gain characteristics of the InGaAsN single-QW and InGaAsN double-QWs.

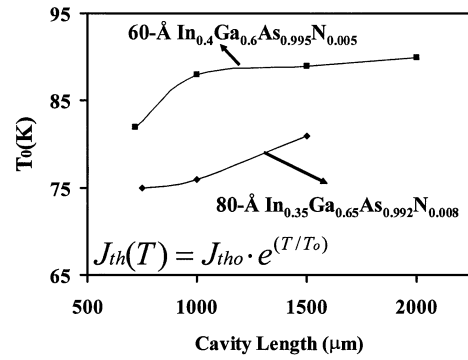


Fig. 11.  $T_0$  comparison for 80-Å In<sub>0.35</sub>Ga<sub>0.65</sub>As<sub>0.992</sub>N<sub>0.008</sub> single-QW and 60-Å In<sub>0.4</sub>Ga<sub>0.6</sub>As<sub>0.995</sub>N<sub>0.005</sub> single-QW lasers, for a temperature range of 20 °C–60 °C.

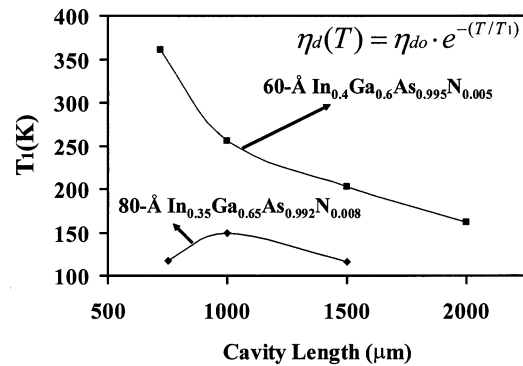


Fig. 12.  $T_1$  comparison for 80-Å In<sub>0.35</sub>Ga<sub>0.65</sub>As<sub>0.992</sub>N<sub>0.008</sub> single-QW and 60-Å In<sub>0.4</sub>Ga<sub>0.6</sub>As<sub>0.995</sub>N<sub>0.005</sub> single-QW lasers, for temperature range of 20 °C–60 °C.

hole confinement for higher N-content InGaAsN QW lasers, which would also lead to a more temperature sensitive current injection efficiency.

## VII. CONCLUSION

High-performance InGaAs and InGaAsN QWs lasers, with emission wavelengths ranging from 1170 to 1315 nm have been realized by MOCVD growth using AsH<sub>3</sub> as the As-precursor.

Low threshold current density and high temperature operation was obtained from 1300-nm InGaAsN single-QW lasers, resulting in superior performance in comparison to conventional 1300-nm InP-based lasers. Despite the high-strain of the InGaAsN QW, double-QW lasers have been demonstrated with excellent scaling in transparency current and material gain. The utilization of a higher N-content InGaAsN QW has indicated possible increased carrier leakage, in comparison to the structures with lower N-content InGaAsN QW active regions. Remaining issues concern the reliability of these active layer materials as well as the extension to longer wavelengths.

#### ACKNOWLEDGMENT

The authors would like to acknowledge helpful technical discussions with Dr. M. R. T. Tan, Dr. D. P. Bour, Dr. S. W. Corzine, Dr. T. Takeuchi, Dr. Y. L. Chang (Agilent Technologies Laboratories, Palo Alto, CA), and technical assistance by AlfaLight, Inc. (Madison, WI).

#### REFERENCES

- [1] M. Kondow, T. Kitatani, S. Nakatsuka, M. C. Larson, K. Nakahara, Y. Yazawa, M. Okai, and K. Uomi, "GaInNAs: A novel material for long wavelength semiconductor lasers," *IEEE J. Select. Topic Quantum Electron.*, vol. 3, pp. 719–730, June 1997.
- [2] J. S. Harris Jr., "Tunable long-wavelength vertical-cavity lasers: the engine of next generation optical networks?," *IEEE J. Select. Topics Quantum Electron.*, vol. 6, pp. 1145–1160, Nov./Dec. 2000.
- [3] S. Sato, "Low threshold and high characteristics temperature 1.3  $\mu\text{m}$  range GaInNA's lasers grown by metalorganic chemical vapor deposition," *Jpn. J. Appl. Phys.*, vol. 39, pp. 3403–3405, June 2000.
- [4] D. A. Livshits, A. Y.A. Yu. Egorov, and H. Riechert, "8 W continuous wave operation of InGaAsN lasers at 1.3  $\mu\text{m}$ ," *Electron. Lett.*, vol. 36, no. 16, pp. 1381–1382, 2000.
- [5] F. Hohnsdorf, J. Koch, S. Leu, W. Stolz, B. Borchert, and M. Druminski, "Reduced threshold current densities of (GaIn)(NA's)GaAs single quantum well lasers for emission wavelengths in the range 1.28–1.38  $\mu\text{m}$ ," *Electron. Lett.*, vol. 35, no. 7, pp. 571–572, 1999.
- [6] M. Kawaguchi, T. Miyamoto, E. Gouardes, D. Schlenker, T. Kondo, F. Koyama, and K. Iga, "Lasing characteristics of low-threshold GaInNA's lasers grown by metalorganic chemical vapor deposition," *Jpn. J. Appl. Phys.*, vol. 40, pp. L744–L746, July 2001.
- [7] T. Takeuchi, Y.-L. Chang, M. Leary, A. Tandon, H.-C. Luan, D. P. Bour, S. W. Corzine, R. Twist, and M. R. Tan, "Low threshold 1.3- $\mu\text{m}$  InGaAsN vertical cavity surface emitting lasers grown by metalorganic chemical vapor deposition," presented at the IEEE LEOS 2001 Post-Deadline Session, San Diego, CA, Nov. 2001.
- [8] N. Tansu and L. J. Mawst, "Low-threshold strain-compensated InGaAs(N) ( $\lambda = 1.19 - 1.31 \mu\text{m}$ ) quantum well lasers," *IEEE Photon. Technol. Lett.*, vol. 14, pp. 444–446, Apr. 2002.
- [9] N. Tansu, N. J. Kirsch, and L. J. Mawst, "Low-threshold-current-density 1300-nm dilute-nitride quantum well lasers," *Appl. Phys. Lett.*, vol. 81, no. 14, pp. 2523–2525, Sept. 2002.
- [10] N. Tansu, A. Quandt, M. Kanskar, W. Mulhearn, and L. J. Mawst, "High-performance and high-temperature continuous-wave-operation 1300-nm InGaAsN quantum well lasers by organometallic vapor phase epitaxy," *Appl. Phys. Lett.*, vol. 83, no. 1, pp. 18–20, July 2003.
- [11] N. Tansu, J. Y. Yeh, and L. J. Mawst, "Experimental evidence of carrier leakage in InGaAsN quantum-well lasers," *Appl. Phys. Lett.*, vol. 83, no. 11, pp. 2112–2114, Sept. 2003.
- [12] —, "Improved photoluminescence of InGaAsN-(In)GaAsP quantum well by organometallic vapor phase epitaxy using growth pause annealing," *Appl. Phys. Lett.*, vol. 82, no. 18, pp. 3008–3110, May 2003.
- [13] J. Wei, F. Xia, C. Li, and S. R. Forrest, "High  $T_0$  long-wavelength InGaAsN quantum-well lasers grown by GSMBE using a solid arsenic source," *IEEE Photon Technol. Lett.*, vol. 14, p. 597, 2002.
- [14] K. D. Choquette, J. F. Klem, A. J. Fischer, O. Blum, A. A. Allerman, I. J. Fritz, S. R. Kurtz, W. G. Breiland, R. Sieg, K. M. Geib, J. W. Scott, and R. L. Naone, "Room temperature continuous wave InGaAsN quantum well vertical-cavity lasers emitting at 1.3  $\mu\text{m}$ ," *Electron. Lett.*, vol. 36, no. 16, pp. 1388–1390, 2000.
- [15] W. Ha, V. Gambin, M. Wistey, S. Bank, S. Kim, and J. S. Harris Jr., "Multiple quantum well GaInNAs-GaNA's ridge-waveguide laser diodes operating out to 1.4  $\mu\text{m}$ ," *IEEE Photon. Technol. Lett.*, vol. 14, May 2002.
- [16] C. S. Peng, T. Jouhti, P. Laukkanen, E.-M. Pavelescu, J. Konttinen, W. Li, and M. Pessa, "1.32- $\mu\text{m}$  GaInNAs-GaAs laser with a low threshold current density," *IEEE Photon. Technol. Lett.*, vol. 14, pp. 275–277, Mar. 2002.
- [17] W. Li, T. Jouhti, C. S. Peng, J. Konttinen, P. Laukkanen, E.-M. Pavelescu, and M. Pessa, "Low-threshold-current 1.32- $\mu\text{m}$  GaInNAs-GaAs single-quantum-well lasers grown by molecular-beam epitaxy," *Appl. Phys. Lett.*, vol. 79, no. 21, pp. 3386–3388, Nov. 2001.
- [18] S. Sato and S. Satoh, "1.21  $\mu\text{m}$  continuous-wave operation of highly strained GaInAs quantum well lasers on GaAs substrates," *Jpn. J. Appl. Phys.*, vol. 38, pp. L990–L992, 1999.
- [19] W. Choi, P. D.P. Daniel Dapkus, and J. J. Jack J. Jewell, "1.2- $\mu\text{m}$  GaAsP/InGaAs strain compensated single-quantum well diode laser on GaAs using metal-organic chemical vapor deposition," *IEEE Photon. Technol. Lett.*, vol. 11, pp. 1572–1574, 1999.
- [20] T. Kondo, D. Schlenker, T. Miyamoto, Z. Chen, M. Kawaguchi, E. Gouardes, F. Koyama, and K. Iga, "Lasing characteristics of 1.2  $\mu\text{m}$  highly strained GaInAsGaAs quantum well lasers," *Jpn. J. Appl. Phys.*, vol. 40, pp. 467–471, Feb. 2000.
- [21] N. Tansu and L. J. Mawst, "High-performance, strain compensated InGaAs-GaAsP-GaAs ( $\lambda = 1.17 \mu\text{m}$ ) quantum well diode lasers," *IEEE Photon. Technol. Lett.*, vol. 13, pp. 179–181, Mar. 2001.
- [22] N. Tansu, Y. L. Chang, T. Takeuchi, D. P. Bour, S. W. Corzine, M. R. T. Tan, and L. J. Mawst, "Temperature analysis and characteristics of highly-strained InGaAs(N)-GaAs-InGaP ( $\lambda > 1.17 \mu\text{m}$ ) quantum well lasers," *IEEE J. Quantum Electron.*, vol. 38, pp. 640–651, June 2002.
- [23] T. Takeuchi, Y.-L. Chang, A. Tandon, D. Bour, S. Corzine, R. Twist, M. Tan, and H.-C. Luan, "Low threshold 1.2  $\mu\text{m}$  InGaAs quantum well lasers grown under low As/III ratio," *Appl. Phys. Lett.*, vol. 80, no. 14, pp. 2445–2447, Apr. 2002.
- [24] F. Bugge, G. Erbert, J. Fricke, S. Gramlich, R. Staske, H. Wenzel, U. Zeimer, and M. Weyers, "12 W continuous-wave diode lasers at 1120 nm with InGaAs quantum wells," *Appl. Phys. Lett.*, vol. 79, no. 13, pp. 1965–1967, Sept. 2001.
- [25] R. Fehse, S. Tomic, A. R. Adams, S. J. Sweeney, E. P. O'Reilly, A. Andreev, and H. Riechert, "A quantitative study of radiative, auger, and defect related recombination processes in 1.3- $\mu\text{m}$  GaInNAs-based quantum-well lasers," *IEEE J. Select. Topics Quantum Electron.*, vol. 8, pp. 801–810, July 2002.
- [26] N. Tansu and L. J. Mawst, "Temperature sensitivity of 1300-nm InGaAsN quantum well lasers," *IEEE Photon. Technol. Lett.*, vol. 14, pp. 1052–1054, Aug. 2002.
- [27] Z. B. Chen, D. Schlenker, F. Koyama, T. Miyamoto, A. Matsutani, and K. Iga, "High temperature characteristics of highly strained 1.2- $\mu\text{m}$  InGaAs/GaAs Lasers," in *Proc. APCCOECC'99*, vol. 2, Beijing, China, 1999, pp. 1311–1314.
- [28] S. Mogg, N. Chitica, R. Schatz, and M. Hammar, "Properties of highly strained InGaAs/GaAs quantum wells for 1.2- $\mu\text{m}$  laser diodes," *Appl. Phys. Lett.*, vol. 81, no. 13, pp. 2334–2336, Sept. 2002.
- [29] R. L. Sellin, C. Ch. Ribbat, M. Grundmann, N. N. Ledentsov, and D. Bimberg, "Close-to-ideal device characteristics of high-power InGaAs/GaAs quantum dot lasers," *Appl. Phys. Lett.*, vol. 78, no. 9, pp. 1207–1209, Feb. 2001.
- [30] A. Stintz, G. T. Liu, H. Li, L. F. Lester, and K. J. Malloy, "Low-threshold current density 1.3- $\mu\text{m}$  quantum-dot lasers with the Dots-in-a-Well (DWELL) structure," *IEEE Photon. Technol. Lett.*, vol. 12, pp. 591–593, June 2000.
- [31] P. M. Smowton, E. Hermann, Y. Ning, H. D. Summers, and P. Blood, "Optical mode loss and gain of multiple-layer quantum-dot lasers," *Appl. Phys. Lett.*, vol. 78, no. 18, pp. 2629–2631, Apr. 2001.
- [32] G. L. Belenky, C. L. Reynolds Jr., D. V. Donetsky, G. E. Shtengel, M. S. Hybertsen, M. A. Alam, G. A. Baraff, R. K. Smith, R. F. Kazarinov, J. Winn, and L. E. Smith, "Role of p-doping profile and regrowth on the static characteristics of 1.3- $\mu\text{m}$  MQW InGaAsP-InP lasers: experiment and modeling," *IEEE J. Quantum Electron.*, vol. 35, pp. 1515–1520, Oct. 1999.
- [33] *Proc. 11th IPRM 1999*, 1999, MoP09.
- [34] N. Tansu and L. J. Mawst, "The role of hole-leakage in 1300-nm InGaAsN quantum well lasers," *Appl. Phys. Lett.*, vol. 82, no. 10, pp. 1500–1502, Mar. 2003.



**Nelson Tansu** was born in Medan, North Sumatra (Indonesia) in October 1977. He received the B.S. degree in applied mathematics, electrical engineering, and physics (AMEP) and the Ph.D. degree in electrical engineering from the University of Wisconsin-Madison, in 1998 and 2003, respectively.

Since July 2003, he has been an Assistant Professor in the Department of Electrical and Computer Engineering, at the P. C. Rossin College of Engineering and Applied Science at Lehigh University, Bethlehem, PA, where he has also been a Faculty Member with the Center for Optical Technologies since July 2003. His research works include design, fabrication and MOCVD growth of novel-active-material GaAs-based vertical cavity lasers (VCSELs) for all practical transmission windows of optical-communications systems; 850-nm VCSELs (InGaAsP QW), 1300-nm diode lasers (InGaAsN QW), and 1550-nm diode lasers. His focus is also on the physics of semiconductor quantum-well lasers encompassing recombination mechanisms, optical gain, carrier transport, and temperature characteristics. His research interest is in the areas of photonics, optoelectronics, nanotechnology, and photonic crystals. Professor Tansu has published widely in numerous refereed international journal and conference publications (*total* > 35), and he currently holds several US patents. He has also given numerous lectures, seminars, and invited talks (*total* > 18) in universities, research institutions, and conferences in the U.S., Canada, Europe, and Asia.

Dr. Tansu was a recipient of the Bohn Scholarship, the WARF Graduate University Fellowship, the Vilas Graduate University Fellowship, and the Graduate Dissertator Travel Funding Award at the University of Wisconsin-Madison. He also received the 2003 Harold A. Peterson ECE Best Research Paper Award (1st Prize) from the University of Wisconsin-Madison.

**Jeng-Ya Yeh** received the B.S. degree in physics from the National Tsing Hua University, Hsinchu, Taiwan in 1996. He is currently working toward the Ph.D. degree in the Department of Electrical and Computer Engineering at the University of Wisconsin-Madison.

He is currently a Research Assistant in the Reed Center for Photonics at the University of Wisconsin-Madison. His primary research interest focuses on developing high-performance long wavelength (1300-nm and beyond) InGaAsN QW lasers by metalorganic chemical vapor deposition (MOCVD) for optical communication. His other research interests include optimization and physical understanding of the lasing characteristics of InGaAsN QW lasers.

**Luke J. Mawst** (M'88–SM'93) was born in Chicago, IL, in 1959. He received the B.S. degree in engineering physics and the M.S. and Ph.D. degrees in electrical engineering from the University of Illinois at Urbana-Champaign, in 1982, 1984, and 1987, respectively. His dissertation research involved the development of index-guided semiconductor lasers and laser arrays grown by MOCVD.

He joined TRW, Inc., Redondo Beach, CA, in 1987, where he was a Senior Scientist in the Research Center, engaged in the design and development of semiconductor lasers using MOCVD crystal growth. He developed a novel single-laser structure, the ARROW laser, as a source for coupling high powers into fibers. He has also been involved in the development of two-dimensional coherent surface-emitting arrays, vertical-cavity surface emitters, and distributed-feedback laser structures. He is currently an Associate Professor at the University of Wisconsin-Madison, where he is involved in the development novel III/V compound semiconductor device structures, including vertical cavity surface emitters (VCSELs), active photonic lattice structures, InGaAsN lasers, and high-power Al-free diode lasers. He has authored or coauthored more than 120 technical papers and holds 15 patents.

Dr. Mawst is the Co-inventor of the Resonant Optical Waveguide (ROW) antiguidded array and has contributed to its development as a practical source of high coherent power, for which he received the TRW Group Level Chairman's Award.